



## MAIN SEQUENCE EVOLUTION WITH LAYERED SEMICONVECTION

KEVIN MOORE<sup>1,2,3</sup> AND PASCALE GARAUD<sup>1</sup>

<sup>1</sup>Department of Applied Mathematics and Statistics, University of California, Santa Cruz, CA, USA

<sup>2</sup>Department of Astronomy & Astrophysics, University of California, Santa Cruz, CA, USA

<sup>3</sup>TASC, University of California, Santa Cruz, CA, USA

Received 2015 May 20; accepted 2015 December 4; published 2016 January 20

### ABSTRACT

Semiconvection is a form of mixing in thermally unstable regions that are partially stabilized by composition gradients. It has the greatest potential impact on the evolution of the cores of main sequence stars in the mass range  $1.2 M_{\odot}$ – $1.7 M_{\odot}$ . We present the first stellar evolution calculations using the new prescription for semiconvective mixing proposed by Wood et al. Semiconvection in stars is predominately layered semiconvection. In our model, the layer height is an adjustable parameter analogous to the mixing length in convection. The rate of mixing inside semiconvective regions is sensitively dependent on the layer height. We find a critical layer height that separates weak semiconvective mixing (where stellar evolution is well-approximated by ignoring semiconvection entirely and using the Ledoux criterion for convection) from strong semiconvective mixing (where all composition gradients are rapidly mixed, so stellar evolution is well-approximated by ignoring them altogether and using the Schwarzschild criterion for convection instead). This critical layer height is much smaller than the minimum layer height derived from simulations so we predict that stellar evolution is nearly the same as in models ran with the Schwarzschild criterion. We also investigate the effects of composition gradient smoothing, finding that it causes convective cores to artificially shrink in the absence of additional mixing beyond the convective boundary. Layered semiconvection with realistic layer heights provides enough such mixing to avoid this problem. Finally, we discuss the potential of detecting layered semiconvection and its implication on convective core sizes in solar-like oscillators.

*Key words:* convection – stars: evolution – stars: interiors

## 1. INTRODUCTION

### 1.1. Convection with Composition Gradients

One of the outstanding challenges in constructing accurate stellar models is understanding macroscopic mixing driven by fluid instabilities. Numerical simulations of these instabilities cannot be used in real time within stellar evolution calculations over an appreciable fraction of a star’s life due to the large separation of length and timescales between the small-scale fluid motions and global stellar behavior. Instead, stellar evolution codes must rely on one-dimensional prescriptions for the transport of energy, composition, and angular momentum associated with instabilities such as convection, overshoot, shear, etc.

Mixing length theory (MLT; Böhm-Vitense 1958) is the standard way of modeling convection in stars and planets, and is usually applied in two steps. First, one determines which regions are convectively stable and unstable, then one adds a model for the convective flux to the total heat flux as well as a model for turbulent mixing in the evolution equation for each chemical species. In the standard MLT, the first of these two steps is done by determining whether a region is linearly stable or unstable to overturning convection through a comparison of the local structural gradients (see also Kippenhahn et al. 2012). Ignoring composition gradients, the presence or absence of convection is established by the *Schwarzschild criterion*, which states that a region is linearly unstable when

$$\frac{3\kappa Pl}{16\pi acGT^4 m} \equiv \nabla_{\text{rad}} > \nabla_{\text{ad}} \equiv \left( \frac{\partial \ln T}{\partial \ln P} \right)_{\text{ad}}, \quad (1)$$

where  $\nabla_{\text{rad}}$  is the radiative temperature gradient (the temperature gradient required if all the energy is transported via photon

diffusion),  $\nabla_{\text{ad}}$  is the adiabatic temperature gradient, computed directly from the equation of state,  $\kappa$  is the opacity,  $P$  is the pressure,  $l$  is the luminosity,  $a$  is the radiative constant,  $c$  is the speed of light,  $G$  is the gravitational constant,  $T$  is the temperature, and  $m$  is the local mass coordinate. To account for composition gradients, the corresponding diagnostic is the *Ledoux criterion* instead (Ledoux 1947), whereby linear instability to overturning convection occurs when

$$\nabla_{\text{rad}} > \nabla_{\text{ad}} + \frac{\phi}{\delta} \nabla_{\mu} \equiv \nabla_L, \quad (2)$$

where  $\phi$  and  $\delta$  are thermodynamic derivatives of the equation of state,

$$\phi = \left( \frac{\partial \ln \rho}{\partial \ln \mu} \right)_{P,T}, \quad \delta = - \left( \frac{\partial \ln \rho}{\partial \ln T} \right)_{P,\mu}, \quad (3)$$

with  $\mu$  being the mean molecular weight of the material, and

$$\nabla_{\mu} = \frac{d \ln \mu}{d \ln P} \quad (4)$$

is the local non-dimensional composition gradient.

Having established in this manner whether a region is stable or unstable to overturning convection, the second step of the process is the application of a model for heat and composition transport. In the standard MLT, the convective heat flux scales as  $F_{\text{conv}} \propto (\nabla - \nabla_{\text{ad}})^{3/2}$ , while compositional mixing is either assumed to be instantaneous or treated as a diffusive process with a diffusion coefficient given by  $D_{\text{conv}} = l_{\text{MLT}} v_{\text{conv}}/3$  where  $l_{\text{MLT}}$  is the mixing length (typically of the order of a pressure scale height), and  $v_{\text{conv}} \propto (\nabla - \nabla_{\text{ad}})^{1/2}$  is the characteristic convective velocity. In what follows, we will

refer to stellar models that use the standard MLT and that are computed using the Schwarzschild criterion as the ‘‘Schwarzschild case’’ or ‘‘Schwarzschild models,’’ and models computed using the Ledoux criterion will be similarly named.

We already note, however, that this basic MLT formalism suffers from a number of shortcomings. First, by deciding whether a region is convective or not based on a linear stability criterion, it ignores the possibility of instability to finite amplitude perturbations (i.e., a subcritical instability). While thermal convection is known not to have any subcritical branch (Joseph 1966), this is not true for thermo-compositional convection (Proctor 1981). Hence, regions that are Ledoux-stable but Schwarzschild-unstable could still be prone to mixing. We shall return to this point shortly. Second, this model ignores non-local effects, such as the overshooting of convective plumes into nearby radiative regions. Overshooting prescriptions must be added a posteriori in MLT models. Third, the application of the standard MLT prescription for turbulent heat transport and turbulent mixing is physically inconsistent with the use of either Schwarzschild or Ledoux criteria. Indeed, it is not consistent with the Ledoux criterion because the convective flux does not drop to zero while approaching the radiative–convective boundary from the convective side. As a result the fluxes are discontinuous across the interface. It is also inconsistent with the use of the Schwarzschild criterion, because MLT assumes that a convection zone is compositionally homogeneous, an assumption which in turn relies on the turbulent diffusion timescale being much shorter than any relevant stellar evolution timescale. While this is usually the case deep within a convective region, it cannot be true near the radiative–convective boundary in models that use the Schwarzschild criterion since the turbulent diffusivity tends toward zero there.

Several of these problems were recently pointed out by Gabriel et al. (2014). They argue that the only consistent way of defining the edge of the convection zone in a stellar evolution calculation is to seek the radius where  $\nabla_{\text{rad}} = \nabla_{\text{ad}}$ , extrapolating both quantities from the convective side of the boundary as needed. This prescription resolves some of the aforementioned issues, is consistent with the standard MLT’s assumption of fully mixed convective regions, and effectively means that there is never any need to distinguish between the use of the Schwarzschild or Ledoux criteria to locate the edge of the convection zone: the Schwarzschild criterion is the only relevant one. However, it still suffers from the problem discussed above, namely that the assumption of a chemically uniform convective zone must fail near its edge. A more physically sound solution would be to modify the MLT to properly model the effect of composition gradients on the efficiency of convection. This involves two distinct questions: (1) how to account for the effects of composition gradients in regions that are Ledoux-unstable, i.e., fully convective, and (2) how to account for the possibility of mixing in regions that are Ledoux-stable but Schwarzschild-unstable. Question (1) is briefly discussed in Section 3, and will be the subject of a separate publication. In all that follows we are now concerned with question (2) only.

### 1.2. Semiconvection

As mentioned above, when the composition gradient is stabilizing ( $\nabla_{\mu} > 0$ , so  $\nabla_{\text{ad}} < \nabla_{\text{L}}$ ) then there can be regions where  $\nabla_{\text{ad}} < \nabla_{\text{rad}} < \nabla_{\text{L}}$  that are linearly stable to convection

under the Ledoux criterion, but would be unstable under the Schwarzschild criterion. First discussed in the context of the evolution of high-mass stars by Schwarzschild & Härm (1958), such regions were named semiconvective. Given the general lack of understanding of their true nature, controversy initially reigned on how to best model them (see the review by Stothers 1970, for instance). Kato (1966) was the first to clarify the problem by showing that semiconvective regions are in fact subject to an entirely different kind of linear instability that is double-diffusive in nature, and sometimes referred to as oscillatory double-diffusive convection (ODDC). As such, it is now typically modeled using prescriptions (to quantify the amount of heat and compositional transport across the semiconvective layer) that are distinct from MLT.

There are a vast number and range of available semiconvective prescriptions (see the review by Merryfield 1995, for instance). Very basic ones merely prescribe the value of the temperature gradient and  $\mu$ -gradient within the semiconvective layer (e.g., Schwarzschild & Härm 1958; Sakashita & Hayashi 1961; Stothers 1970; Robertson & Faulkner 1972; Stothers & Chin 1975). First-order models treat mixing using semiconvection as a diffusive process, and propose relatively simple formulae for the semiconvective heat flux and for the turbulent compositional diffusivity (e.g., Stevenson 1979; Langer et al. 1983; Spruit 1992, 2013). Finally, second-order (or even higher-order) closure models which involve the solution of a set of nonlinear equations for the Reynolds stresses and the turbulent fluxes have been proposed (e.g. Grossman & Taam 1996; Canuto 1999; Ding & Li 2014). Inevitably, however, all of these models rely on one or more ad-hoc prescriptions, for the gradients, for the diffusion coefficients, and for the closure assumptions respectively. Their validation against experimental data is therefore crucial should one wish to build confidence in their predictive capabilities.

Unfortunately, it is practically impossible to test a semiconvection model directly. Laboratory experiments can only be done with fluids that have relatively large Prandtl numbers (the Prandtl number is the ratio of the kinematic viscosity to the thermal diffusivity), of the order of one or larger, while the interiors of stars on the main sequence typically have Prandtl number of the order of  $10^{-5}$  or smaller (Garaud et al. 2015). Among other important consequences this implies that while semiconvective regions are linearly unstable to ODDC at astrophysical parameters, they nearly always require finite amplitude perturbations in the geophysical context (see Section 2 for detail). The dynamics resulting from the instabilities are therefore also fundamentally different, which raises the uncomfortable question of whether any of the results reported in the vast geophysical literature on ODDC (see the reviews by Turner 1973; Radko 2013) actually apply to stellar semiconvection.

Until recently, the only alternative available to assess the quality of various semiconvective prescriptions was to implement them in stellar evolution codes, and determine whether the resulting models provided a better or worse fit to the available data. Such attempts have been made (e.g., Langer & Maeder 1995; Silva Aguirre et al. 2011; Sukhbold & Woosley 2014; Georgy et al. 2015) but the interpretation of the results, however, is so strongly dependent on a number of other model uncertainties (such as the possibility of any other kind of mixing due to shear, overshoot, MHD instabilities, the

effects of rotation, or simply uncertainties on the stellar ages or internal composition), that the robustness of the conclusions is unavoidably doubtful.

In the last few years, however, numerical experiments using three-dimensional Direct Numerical Simulations (3D DNSs) in parameter regimes that are somewhat closer to the stellar regime (namely, at low Prandtl number) have finally become possible. These can be used as direct tests of existing semiconvective prescriptions, and preliminary results at Prandtl numbers down to about  $10^{-2}$  already cast serious doubts about their validity. Indeed, as shown by Rosenblum et al. (2011) and studied by Mirouh et al. (2012), Wood et al. (2013) and Moll et al. (2015), there are two distinct forms of semiconvection: layered semiconvection, and non-layered semiconvection, found in regions that have weaker (resp. stronger) composition gradients. Furthermore, Moll et al. (2015) have found that there are two types of layered semiconvection: one where layers spontaneously form, and one in which layers can only form through finite amplitude instabilities. Transport through either form of layered convection, and through non-layered systems, is vastly different, so a complete semiconvection prescription should first establish which of these three forms is expected and then propose flux laws for each case separately. This has now been done, with a new theory for semiconvective layer formation in astrophysics explicitly laid out by Mirouh et al. (2012), and preliminary empirical flux laws for layered and non-layered semiconvection measured from low Prandtl number 3D DNSs by Wood et al. (2013) and Moll et al. (2015). We now turn to the question of testing the implications of this new semiconvective model for stellar evolution theory.

While semiconvection was historically used in modeling high-mass stars with  $M \geq 10 M_{\odot}$  (Schwarzschild & Härm 1958; Stothers 1970; Stothers & Chin 1975; Langer et al. 1985), we choose to focus on the simplest stellar models where we can investigate the effects of semiconvective mixing—main sequence stars slightly more massive than the Sun. Indeed, semiconvective mixing in main sequence stars is typically encountered during convective core burning, just outside of the region that is Ledoux-unstable to convection. It is caused by the buildup of composition gradients induced by the long tail of low-temperature proton–proton chain burning that extends outside of the convective core. For main sequence stars in the mass range  $1.2 M_{\odot}$ – $1.7 M_{\odot}$ , the convective cores are so small that the composition gradient immediately outside the convective region is large enough to significantly change the core mass between the Ledoux and Schwarzschild criteria (see Section 4.1). The effect of semiconvection on these stars has already been investigated (Faulkner & Cannon 1973; Gabriel & Noels 1977; Crowe & Mitalas 1982; Silva Aguirre et al. 2010b), but not using prescriptions motivated by numerical simulations. It is nevertheless known to affect the convective core mass and its evolution with time, and as a result, the age at which the star leaves the main sequence. Since asteroseismology now enables us to detect with some accuracy the size of convective cores in main sequence stars (Mazumdar et al. 2006; Cunha & Metcalfe 2007; Silva Aguirre et al. 2010a; Brandão et al. 2014), one may hope in the near future to be able to constrain semiconvective models using asteroseismic data. For these reasons, we are interested in establishing (1) what are the mass ranges where the cores of main sequence stars are most sensitive to semiconvection and (2) what is the effect of the new layered semiconvective prescription proposed by

Wood et al. (2013) on the evolution of the convective core mass in these stars. To answer these questions, we have implemented the new Wood et al. (2013) layered semiconvection prescription into the open-source stellar evolution code MESA<sup>4</sup> (Paxton et al. 2011, 2013, 2015).

We review the general properties of the Wood et al. (2013) model in Section 2. We argue that ODDC most likely takes the form of layered semiconvection where layers form spontaneously for parameters representative of stellar interiors (see also Garaud et al. 2013), with the layer height remaining a free parameter. Section 3 details how we implement this mixing prescription in MESA. It also discusses the effects of numerical smoothing on convective core evolution. Section 4 presents applications of this theory to the growth of convective cores in main sequence stars and identifies the stellar mass range which is most sensitive to the effects of semiconvection. We show the effects of varying layer heights on convective core growth, and derive a critical layer height for semiconvective regions to persist throughout the main sequence. We summarize our conclusions in Section 5 and briefly outline future directions of investigation into semiconvective mixing.

## 2. OSCILLATORY DOUBLE-DIFFUSIVE CONVECTION

As discussed in Section 1, oscillatory double diffusive convection is a mild form of convection that occurs in the presence of stabilizing chemical gradients and destabilizing thermal gradients. The onset and strength of ODDC is controlled by several dimensionless parameters. The first is the Prandtl number,

$$\text{Pr} = \frac{\nu}{\kappa_T}, \quad (5)$$

where  $\nu$  is the microscopic kinematic viscosity and  $\kappa_T$  is the thermal diffusivity (both with units of  $\text{cm}^2 \text{s}^{-1}$  in cgs units). As discussed in Section 1, low Prandtl numbers ( $\approx 10^{-8}$ – $10^{-3}$ ) are typical in stars and gas giant planets, while telluric planet interiors may have  $\text{Pr} > 1$  (Soderlund et al. 2013). The second parameter is the diffusivity ratio,

$$\tau = \frac{\kappa_{\mu}}{\kappa_T}, \quad (6)$$

of the microscopic compositional diffusivity  $\kappa_{\mu}$ , to the thermal diffusivity. ODDC only occurs when  $\tau < 1$ , which is the standard situation in stars since heat is transported via photon diffusion as well as collisions between nuclei, while chemical species only diffuse through collisional processes. Finally, the third parameter is the density ratio

$$R_0 = \frac{\delta(\nabla - \nabla_{\text{ad}})}{\phi \nabla_{\mu}}, \quad (7)$$

where  $\delta$  and  $\phi$  are the equation of state derivatives defined in the previous section (with  $\delta = \phi = 1$  for an ideal gas). As discussed by Baines & Gill (1969), semiconvection occurs when

$$R_{\text{crit}} < R_0 < 1, \quad (8)$$

<sup>4</sup> Version 6794.

where

$$R_{\text{crit}} = \frac{\text{Pr} + \tau}{\text{Pr} + 1}. \quad (9)$$

Equation (8) is a local criterion, analogous to the Schwarzschild and Ledoux criteria used to determine convective instability. It can be rewritten in terms of  $\nabla$  as

$$\nabla_{\text{ad}} + R_{\text{crit}} \frac{\phi}{\delta} \nabla_{\mu} < \nabla < \nabla_{\text{ad}} + \frac{\phi}{\delta} \nabla_{\mu}. \quad (10)$$

Regions with  $R_0 > 1$  ( $\nabla > \nabla_{\text{ad}} + \frac{\phi}{\delta} \nabla_{\mu}$ ) are unstable to convection, while regions with  $R_0 < R_{\text{crit}}$  ( $\nabla < \nabla_{\text{ad}} + R_{\text{crit}} \frac{\phi}{\delta} \nabla_{\mu}$ ) are stable and therefore radiative. We see that for high Prandtl number but small diffusivity ratio fluids (which is the case for nearly all geophysical fluids),  $R_{\text{crit}} \simeq 1$ , implying that the region of parameter space linearly unstable to ODDC is very small. This implies that nearly all instances of ODDC in geophysical flows arise from finite-amplitude perturbations rather than infinitesimal perturbations. By contrast, for  $\text{Pr}, \tau \ll 1$  we have  $R_{\text{crit}} \rightarrow 0$ , so the criterion for linear ODDC instability, that is, instability to *infinitesimal* perturbations, is nearly identical to the semiconvective criterion that is typically employed in modeling stars,  $\nabla_{\text{ad}} < \nabla < \nabla_{\text{ad}} + \frac{\phi}{\delta} \nabla_{\mu}$ .

For low Prandtl number fluids, the region of parameter space unstable to ODDC is itself divided into two distinct domains, one in which ODDC spontaneously transitions into a layered state, and one in which it does not. The layering transition was shown by Rosenblum et al. (2011) and Mirouh et al. (2012) to be caused by the  $\gamma$ -instability, a mean-field instability first discussed in the geophysical context of fingering convection by Radko (2003). The  $\gamma$ -instability normally only operates under certain conditions (see Mirouh et al. 2012, for details), hence the division of parameter space into regions that spontaneously transform into layers, and those that do not. Interestingly, we find that stellar semiconvective zones that are adjacent to fully convective regions always fall into the former category. In what follows, we therefore ignore the possibility of non-layered semiconvection.

Layered semiconvection takes the form of fully convective layers of height  $H_L$ , separated by thin, stably stratified interfaces. As shown by Wood et al. (2013), at low Prandtl number and in the regime where layers form spontaneously (which is the only one considered here) the interfaces are quite turbulent (contrary to the assumptions of the model of Spruit 1992), constantly sheared and distorted by traveling interfacial gravity waves that interact with the convective eddies within the layers. The latter tend to merge rapidly with one another as time evolves, and  $H_L$  gradually grows with time. Whether the merger process would continue indefinitely or eventually stop once a certain equilibrium layer height is achieved remains to be determined. Nevertheless, in what follows we assume it exists and treat this ultimate layer height as a free parameter of the model, much like the mixing length in standard MLT.

The total heat flux at a given location in a star can be expressed as the sum of the radiative and semiconvective heat fluxes,

$$F_{\text{tot}} = F_{\text{rad}} + F_{\text{semi}}, \quad (11)$$

where the radiative heat flux is given by

$$F_{\text{rad}} = -k_{\text{rad}} \frac{dT}{dr}, \quad (12)$$

(where  $r$  is the radial coordinate and  $k_{\text{rad}} = \rho c_p \kappa_T$  is the microscopic thermal conductivity with  $c_p$  the specific heat at constant pressure) and the semiconvective heat flux is given by

$$F_{\text{semi}} = -k_{\text{rad}} (\text{Nu}_T - 1) \left( \frac{dT}{dr} - \frac{dT}{dr} \Big|_{\text{ad}} \right), \quad (13)$$

which defines  $\text{Nu}_T$  as the thermal Nusselt number (see below). Similarly, the turbulent compositional flux is written as

$$F_{\mu} = -\kappa_{\mu} (\text{Nu}_{\mu} - 1) \frac{d\mu}{dr}, \quad (14)$$

where  $\text{Nu}_{\mu}$  is the compositional Nusselt number, and

$$\frac{dT}{dr} \Big|_{\text{ad}} = \frac{T}{P} \frac{dP}{dr} \nabla_{\text{ad}}. \quad (15)$$

Wood et al. (2013) ran a systematic set of 3D DNSs of layered semiconvection to measure the Nusselt numbers  $\text{Nu}_T$  and  $\text{Nu}_{\mu}$  as functions of the model parameters  $R_0$ ,  $\text{Pr}$ ,  $\tau$ , and  $H_L$ . Computational resources allowed simulations down to  $\text{Pr}, \tau = 0.01$ . As discussed above, such low values are necessary to have some degree of confidence in the required extrapolation of the results further down to stellar parameters (see Moll et al. 2015, for a discussion of the caveats associated with this extrapolation). Wood et al. (2013) found that both Nusselt numbers vary only weakly with  $R_0$ , and depend on  $H_L$  only through the Rayleigh number,  $\text{Ra}$ , given by

$$\text{Ra} = \left| \frac{\delta}{\rho} \frac{dP}{dr} \left( \frac{d \ln T}{dr} - \frac{d \ln T_{\text{ad}}}{dr} \right) \frac{H_L^4}{\kappa_T \nu} \right|. \quad (16)$$

Empirical fits to the data suggest that  $\text{Nu}_T - 1 = f(R_0, \tau) \text{Ra}^a \text{Pr}^b$ , with  $a = 0.34 \pm 0.01$ ,  $b = 0.34 \pm 0.03$  and where  $f(R_0, \tau)$  is a very weakly varying function of  $R_0$  and  $\tau$  which, among all simulations available to date, is more or less constant and equal to about 0.1. In what follows, we therefore take

$$\begin{aligned} \text{Nu}_T - 1 &= f(R_0, \tau) \text{Ra}^a \text{Pr}^b \\ &\approx 0.1 \text{Ra}^{1/3} \text{Pr}^{1/3}. \end{aligned} \quad (17)$$

Wood et al. (2013) approximated the exponents  $a$  and  $b$  with the fraction  $1/3$ , which is consistent with the standard flux law for interfacial transport (Turner 1973),  $\text{Nu}_T - 1 \propto \Delta T^{4/3}$ , where  $\Delta T = (dT/dr - dT_{\text{ad}}/dr)H_L$  is the mean temperature jump from one layer to the next. This flux law is commonly derived from simple dimensional analysis arguments (Radko 2013), and is therefore expected to hold in this case as well. For the composition transport, the numerical results suggest that  $\text{Nu}_{\mu} - 1 = g(R_0, \tau) \text{Ra}^c \text{Pr}^d$ , with  $c = 0.37 \pm 0.01$ ,  $d = 0.27 \pm 0.04$ , and where  $g(R_0, \tau)$  is also a weakly varying function of  $R_0$  and  $\tau$  as well, this time consistent with  $g \propto 0.03\tau^{-1}$  for the range of simulations available. In what follows, we therefore take:

$$\begin{aligned} \text{Nu}_{\mu} - 1 &= g(R_0, \tau) \text{Ra}^c \text{Pr}^d \\ &\approx 0.03 \tau^{-1} \text{Ra}^{0.37} \text{Pr}^{1/4}. \end{aligned} \quad (18)$$

The next section details how this mixing prescription is actually implemented in MESA.

We note that the scaling laws (17) and (18) are similar—but not identical—to the ones advocated by the new theoretical model of Spruit (2013) for mixing in layered semiconvection. His expression for  $\text{Nu}_T$  is essentially the same as ours, but his expression for  $\text{Nu}_\mu$  would be expressed as  $\text{Nu}_\mu - 1 = R_0 \tau^{-1/2} (\text{Nu}_T - 1)$  in our notation. While we do not have enough data to test the dependence of  $\text{Nu}_\mu$  on  $R_0$  (see the discussion by Wood et al. 2013, for detail), the dependence on  $\tau$  inferred by Wood et al. (2013) is different from the one advocated by Spruit (2013). We also note a slight difference in the exponents of  $\text{Ra}$  and  $\text{Pr}$ , although in this case again we do not have enough data to determine with certainty which model fares best.

### 3. IMPLEMENTATION IN MESA

#### 3.1. MLT and Semiconvection in MESA

MESA is a one-dimensional Lagrangian code that solves the equations of stellar structure in a fully coupled (unsplit) method, although options to split the mixing equations from the burning and structure equations exist. The two equations that are directly affected by the addition of extra mixing are the equations for thermal and compositional transport. The first is discretized as

$$T_{k-1} - T_k = \overline{dm}_k \left[ \nabla_k \left( \frac{dP}{dm} \right) \frac{\overline{T}_k}{\overline{P}_k} \right], \quad (19)$$

where  $T_k$  is the temperature at the center of cell  $k$ ,  $\overline{T}_k$  is the mass-interpolated temperature at the outer face of cell  $k$  (similar for pressures  $P_k$  and  $\overline{P}_k$ ),  $\overline{dm}_k$  is the mean mass of cells  $k$  and  $k-1$ , and  $\nabla_k$  is the temperature gradient at the face of cell  $k$  (cell indices in MESA increase inward toward the core). While not explicit in this equation, the semiconvective prescription directly affects the calculation of the local temperature gradient,  $\nabla$  (see Section 3.1.2 below). The equation of compositional transport, on the other hand, is

$$X_{i,k-1}(t + \delta t) - X_{i,k}(t) = \frac{dX_{i,k}}{dt} \delta t + (F_{i,k+1} - F_{i,k}) \frac{\delta t}{dm_k}, \quad (20)$$

where  $\delta t$  is the time step and

$$F_{i,k} = (X_{i,k} - X_{i,k-1}) \frac{D_k}{dm_k} \quad (21)$$

is the flux of the  $i$ th species through the outer face of the  $k$ th cell,  $D_k$  is the compositional diffusion coefficient, and  $X_{i,k}$  is the mass fraction of the  $i$ th species in the  $k$ th cell; see Section 6.2 in Paxton et al. (2011) for a more detailed discussion. In this case, semiconvective mixing directly affects the calculation of  $D_k$ .

The mixing type of a given cell is determined entirely locally, with regions labeled as semiconvective when

$$\nabla_{\text{ad}} < \nabla_{\text{rad}} < \nabla_{\text{ad}} + \frac{\phi}{\delta} \nabla_\mu. \quad (22)$$

Regions are convective (under the Ledoux criterion) when

$$\nabla_{\text{ad}} + \frac{\phi}{\delta} \nabla_\mu < \nabla_{\text{rad}}. \quad (23)$$

#### 3.1.1. MLT in MESA

The temperature gradient and compositional diffusion coefficients are calculated from the standard equations of MLT in convective regions, as described in Paxton et al. (2011; see also Weiss et al. 2004). We reiterate two problems with such local implementations of MLT in the presence of composition gradients or discontinuities: (1) the convective flux scales as  $F_{\text{conv}} \propto (\nabla - \nabla_{\text{ad}})^{3/2}$ , so it cannot go to zero when  $\nabla = \nabla_{\text{L}}$  at the convective-semiconvective boundary, and (2) the presence of compositional discontinuities can lead to convective cores where  $\nabla \neq \nabla_{\text{ad}}$  at the convective boundary (or  $\nabla \neq \nabla_{\text{L}}$  at the semiconvective boundary), as pointed out by Gabriel et al. (2014). These issues are relevant to any stellar models that are computed using standard local MLT prescriptions. As discussed in the introduction, addressing them in proper detail requires a reformulation of the MLT equations that include composition gradients, which is beyond the scope of this paper. While the local MLT has its limitations, we will see that the main conclusions of this paper are not affected by them.

#### 3.1.2. Semiconvective Temperature Gradient

As in standard MLT, we use the relationship between the heat flux and  $\nabla$  to solve for the latter. Combining Equations (13), (16), and (17) and using our fiducial parameters ( $a = b = 1/3$ ), we rewrite the semiconvective flux as

$$F_{\text{semi}} = 0.1 \frac{T \rho^2 c_P g \kappa_T^{1/3}}{P} \left| \frac{\delta \rho g^2}{P} \right| \times (\nabla - \nabla_{\text{ad}}) H_{\text{L}}^4 |^{1/3} (\nabla - \nabla_{\text{ad}}), \quad (24)$$

where  $g = Gm/r^2$  is the local gravitational acceleration. Dividing Equation (11) by  $k_{\text{rad}} T \rho g / P$  yields

$$\nabla_{\text{rad}} = \nabla + \nabla_{\text{semi}}, \quad (25)$$

where

$$\nabla_{\text{semi}} \equiv - \frac{F_{\text{semi}}}{k_{\text{rad}} T} \left( \frac{d \ln P}{dr} \right)^{-1} = \frac{P}{T \rho g k_{\text{rad}}} F_{\text{semi}}. \quad (26)$$

Equation (25) is a fourth-order polynomial equation in  $\nabla$  so it could in principle be solved analytically for the latter. However, the expression of the solution is too complicated to be of practical value. Instead, we solve it numerically as part of the Newton solver step to advance the star in time. The Jacobian for this Newton solve also requires partial derivatives of  $\nabla$  with respect to local stellar variables, such as  $P$ ,  $T$ ,  $m(r)$ , etc. We calculate these by differentiating Equation (25) implicitly.

#### 3.1.3. Semiconvective Compositional Mixing Coefficient

The compositional mixing rate is locally determined by the semiconvective diffusion coefficient,  $D_{\text{semi}}$ . Its value in layered semiconvection is given by similarly substituting Equation (18) into  $D_{\text{semi}} = \kappa_\mu (\text{Nu}_\mu - 1)$ , which gives, for our fiducial

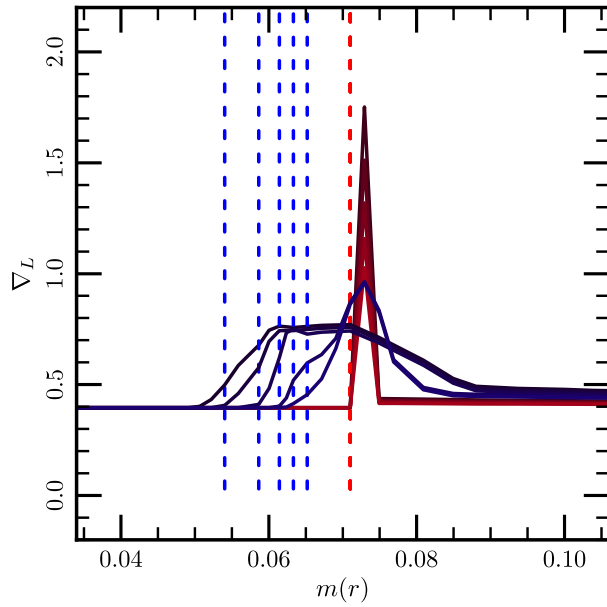


**Figure 1.** Evolution of  $\nabla_L$  profiles of a  $1.5 M_\odot$  star when smoothing is suddenly turned on during evolution on the main sequence. Profiles of  $\nabla_L$  as a function of mass coordinate are shown for five consecutive models where  $\nabla_\mu$ -smoothing is turned off, as well as five consecutive models after  $\nabla_\mu$ -smoothing is enabled. The extent of the convective core is shown by the dashed lines and is constant in mass coordinate until  $\nabla_\mu$ -smoothing is turned on, after which the outer mass coordinate of the convective core moves inward as the composition gradient pushes into the formerly convective region.

parameters ( $c = 0.37$ ,  $d = 1/4$ ),

$$D_{\text{semi}} = 0.03 \frac{\kappa_T^{0.38}}{\nu^{0.12}} \left| \frac{\delta \rho g^2}{P} (\nabla - \nabla_{\text{ad}}) H_L^4 \right|^{0.37}, \quad (27)$$

and is calculated once  $\nabla$  is known. As with  $\nabla$ , partial derivatives of  $D_{\text{semi}}$  are necessary for the Jacobian, which are computed by differentiating Equation (27).

### 3.2. Effects of Composition Gradient Smoothing on Convective Boundaries

Use of the Ledoux criterion can be complicated by small-scale composition gradients that vary greatly from cell to cell. Originally due to concerns over having smooth Brunt–Väisälä frequency values for pulsation mode calculations, MESA smooths  $\nabla_\mu$  using a Gaussian smoothing formula with a 7-cell window by default. This kind of smoothing can have significant, but artificial effects on stellar evolution. Indeed, in core-convective stars, there is usually a sharp jump in composition between the outermost convective cell and the cell immediately above it. This produces a spike in  $\nabla_\mu$  which grows in time, and is the main reason why in the absence of smoothing or any kind of mixing beyond the convective boundary (i.e., without any overshoot or semiconvective mixing), convective cores do not grow as large in the Ledoux case compared with the Schwarzschild case. If this spike is smoothed before the MLT module computes the convective boundaries, then the region of high- $\nabla_\mu$  is artificially spread

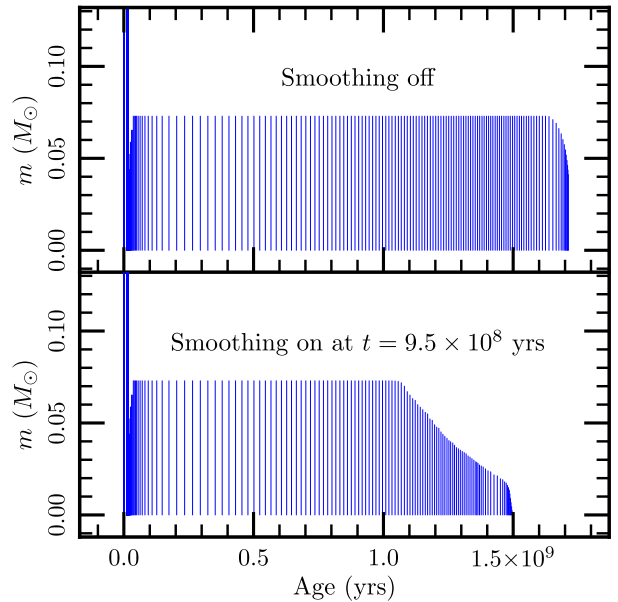


**Figure 2.** Comparison of the effect of  $\nabla_\mu$ -smoothing on the convective core evolution of a  $1.5 M_\odot$  star. The top panel shows a Kippenhahn diagram of evolution under the Ledoux criterion without semiconvection, overshooting, or  $\nabla_\mu$ -smoothing, where the vertical lines mark the extent of convective regions at each time step. The bottom panel shows the evolution of the same star, but with  $\nabla_\mu$ -smoothing turned on suddenly (as in Figure 1) when the core hydrogen mass fraction drops below 0.4, which occurs at  $t = 9.5 \times 10^8$  years. As soon as  $\nabla_\mu$ -smoothing is turned on, the core begins to shrink at a near constant number of cells per step. The apparent delay in core shrinkage in mass coordinate is merely due to the increased spatial resolution near the convective boundary.

inward into cells that used to be convective. This then causes the convective boundary to move inward relative to that of a run which performs the same steps without compositional gradient smoothing.

Figure 1 shows the evolution of a compositional discontinuity at the convective boundary in a numerical experiment in which compositional smoothing is suddenly switched on during the main sequence. This clearly illustrates how the spike in  $\nabla_\mu$  that had built up at the convective boundary starts to diffuse inward when smoothing is turned on, causing the convective boundary to artificially move inward with it. Figure 2 shows a Kippenhahn diagram of a similar run, as well as that of a star where no smoothing was used. As soon as smoothing is enabled, the convective core starts moving inward, resulting in a significantly smaller convective core for the remainder of the main sequence compared to the run without smoothing. This effect occurs for *all* stars that develop a convective core—not just stars that show a strong difference between their evolution under the Ledoux and Schwarzschild criteria; smoothing  $\nabla_\mu$  always shrinks a convective core relative to the same model without smoothing. We consider this to be an artificial effect and our models are run without  $\nabla_\mu$ -smoothing, unless otherwise noted. We will see in Section 4 that this distinction is rendered moot when layered semiconvection is accounted for because of the mixing that naturally occurs beyond the convective boundary.

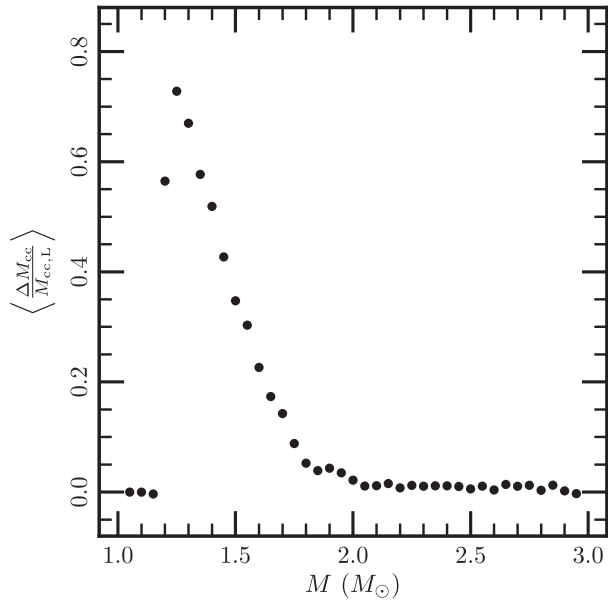


**Figure 3.** Measure of potential impact of semiconvection on the cores of main sequence stars of varying masses, as described in the main text. Core convection occurs for stars with  $M \geq 1.2 M_{\odot}$ , and the larger the computed ratio is, the larger the potential effect of semiconvection on the evolution of the core of the star. A small window exists from  $M \approx 1.2$ – $1.7 M_{\odot}$  where there is a large enough composition gradient outside the convection zone for semiconvection to have a significant impact on the star. See Figure 4 for an illustration of the composition gradients in selected stars.

#### 4. APPLICATIONS TO STELLAR EVOLUTION

##### 4.1. Impact of Semiconvection on the Core Evolution in Low Mass Stars

As discussed in Section 1, semiconvective mixing only occurs in the presence of both stable composition gradients and unstable thermal gradients, which are typically found in regions adjacent to convective zones. The most natural source of stabilizing composition gradients is nuclear burning, and convective burning cores exist in main sequence stars (with  $M \geq 1.2 M_{\odot}$ ) as well as during core helium burning.

In order to best understand the effects of our new semiconvective mixing prescription on the evolution of the size of convective cores, we first identify stars in which it may have a large effect. Figure 3 shows a measure of the potential impact of semiconvection on the core evolution of main sequence stars in the 1– $3 M_{\odot}$  range. We quantify this impact by comparing the predicted convective core sizes computed without semiconvection (and without smoothing, see above) under the Schwarzschild and Ledoux criteria, respectively. Because the Schwarzschild criterion does not take into account composition gradients while the Ledoux criterion does, we expect the sizes of convective cores calculated in the Schwarzschild case to be larger than in the Ledoux case in the presence of stabilizing composition gradients. How much larger will depend on the size of  $\nabla_{\mu}$  outside the convective core, which in turn depends on the local nuclear burning rates and varies with stellar mass. Any semiconvective region, should it exist, must necessarily reside in between the Schwarzschild and Ledoux core boundaries. Its maximum extent is therefore well approximated by the difference between

the two radii, which can be used as a proxy for the potential impact of semiconvection on core evolution.

Figure 3 shows the time-averaged ratio of the difference in convective core mass between the Schwarzschild and Ledoux cases, scaled to that of the Ledoux case, computed as

$$\left\langle \frac{\Delta M_{cc}}{M_{cc,L}} \right\rangle = \frac{1}{\tau_{ms} - \tau_0} \int_{\tau_0}^{\tau_{ms}} \frac{M_{cc,S} - M_{cc,L}}{M_{cc,L}} dt, \quad (28)$$

where  $M_{cc,S}$  is the convective core mass obtained using the Schwarzschild criterion,  $M_{cc,L}$  is the convective core mass obtained using the Ledoux criterion, and the interval  $[\tau_0, \tau_{ms}]$  spans the period between the onset of core convection, and the end of the main sequence. Since this ratio is calculated from two different stellar models, the upper bound on the integral is taken to be the shortest lifetime—here the Ledoux model due to the smaller convective core. The advantage of this measure is that it does not depend at all on the semiconvective prescription employed, but merely probes which main sequence stars have significant chemical gradients outside of their convective cores. Figure 3 shows that the most favorable mass range to explore the effects of semiconvection on the cores of main sequence stars is  $M \approx 1.2$ – $1.7 M_{\odot}$ . We have performed these calculations on stars with masses up to  $30 M_{\odot}$  without seeing another window where semiconvective mixing has a significant impact on convective core evolution during the main sequence.

The significance of the mass range 1.2– $1.7 M_{\odot}$  for semiconvection is best understood by looking at the composition gradient generated by nuclear burning outside the convective core. Figure 4 shows the difference between stars that are susceptible to semiconvection according to the criterion discussed earlier (1.3  $M_{\odot}$  and 1.5  $M_{\odot}$  models), and a 2.8  $M_{\odot}$  model which is not. The relatively weak temperature dependence of the proton–proton chain allows burning to occur in regions outside of the convective core at a rate which gradually drops with radius due to the temperature and density decreasing outward. This radius-dependent burning rate causes the development of a composition gradient which steepens inward. While all stars in the mass range shown in Figure 3 have nearly the same  $\mu$ -profile outside their core for a given age, the position of the edge of the core is strongly dependent on the stellar mass and is located at radii with stronger or weaker  $\mu$ -gradients. Lower-mass stars with smaller convective cores have larger  $\mu$ -gradients just outside their cores, while larger-mass stars with larger cores have correspondingly weaker  $\mu$ -gradients. This is why semiconvection can make the largest difference in the evolution with stars having the smallest convective cores.

Note that higher-mass stars, for which  $\langle \Delta M_{cc}/M_{cc,L} \rangle$  is very low, are not necessarily free of semiconvection. This is because semiconvective regions that are not connected to the convective core will not show up in this diagnostic. In fact semiconvective envelopes that are disconnected from the core are often seen in models of high-mass stars (see e.g., Langer 1991), and the overall effects of semiconvection during more evolved phases can be quite complicated (Sukhbold & Woosley 2014).

Stars may also be susceptible to semiconvection during core helium burning phases. However, helium burning reactions are much more temperature sensitive and do not extend far out of the convective core. As a result, there is not a large difference between the sizes of convective cores calculated under different

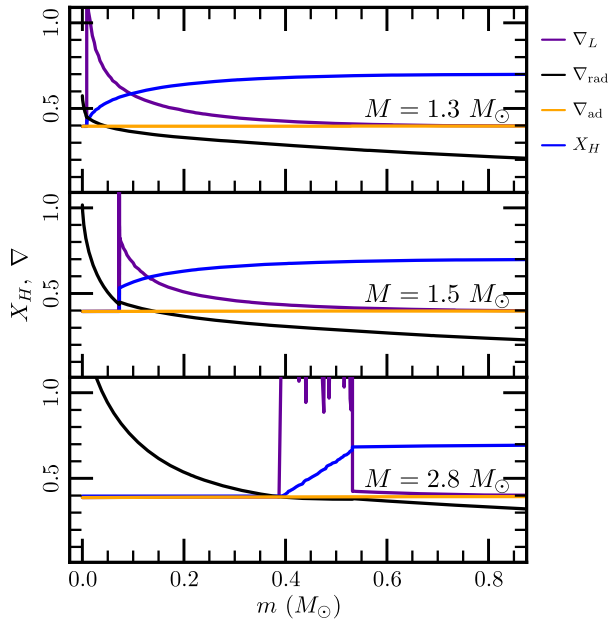


**Figure 4.** Profiles of composition gradients  $\nabla_L$  (purple), radiative gradient  $\nabla_{\text{rad}}$  (black), adiabatic gradient  $\nabla_{\text{ad}}$  (orange), and mass fractions of hydrogen ( $X_H$ , blue), as a function of mass coordinate for stars that can have large semiconvective regions ( $1.3 M_\odot$  and  $1.5 M_\odot$ ) as well as a  $2.8 M_\odot$  star that cannot support significant semiconvection outside of its core. These profiles are obtained by evolving each star under the Ledoux criterion until the central mass fraction of hydrogen first drops below 0.4. The source of the mass-dependence in where semiconvection can occur comes from the size of the composition gradient term in  $\nabla_L$  immediately outside the convective cores. Large values of  $\nabla_L$  outside small convective cores in stars in the mass range  $1.2\text{--}1.7 M_\odot$  cause a significant difference between the convective boundaries determined by the Ledoux and Schwarzschild criteria: the former is the position of the  $\nabla_L$  spike, located at  $m/M_\odot = 0.01, 0.07,$  and  $0.38$ , respectively. The latter is the position where  $\nabla_{\text{rad}} = \nabla_{\text{ad}}$ , located at  $m/M_\odot = 0.04, 0.14,$  and  $0.38$ , respectively. For higher mass stars such as the  $2.8 M_\odot$  case shown, the composition gradient outside the core is too small to allow for large semiconvective regions.

convective criteria. A composition gradient can also exist outside of the hydrogen burning shell due to the less temperature-sensitive proton–proton chain burning outside of the main CNO burning region, but this effect is much less dramatic than during the main sequence due to the higher temperatures in the burning regions, and to the much shorter remaining stellar lifetime. We defer a discussion of the impact of semiconvective mixing on the later stages of high-mass stars to a future paper.

#### 4.2. Maintaining a Composition Gradient

In order for semiconvective regions to persist for significant periods of time, their turbulent mixing rates cannot be too large, otherwise the composition gradient that causes them to exist will be destroyed. If this happens, the semiconvective region is simply converted into a convective region since it is by definition Schwarzschild-unstable. The efficiency of compositional mixing in semiconvective regions is determined by the size of the diffusion coefficient  $D_{\text{semi}}$  (see Equation (27)) and therefore by the layer height  $H_L$ —larger layer heights imply larger diffusion coefficients. This suggests that stellar models with layered semiconvection can be split into three groups—(a) one in which the compositional mixing is so weak it can be neglected altogether, (b) one in which the convective core size

is modified, but the mixing is slow enough for the semiconvective regions to persist throughout the main sequence, and (c) one where the compositional mixing is fast enough to turn semiconvective zones into convective zones over a timescale much shorter than the main sequence lifetime. We anticipate the existence of a critical layer height,  $H_{L,\text{crit}}$ , such that evolution with  $H_L \gg H_{L,\text{crit}}$  (case (c)) is similar to one without semiconvection, but where the edge of the convective zone is determined by the Schwarzschild criterion. Meanwhile, if  $H_L \ll H_{L,\text{crit}}$  (case (a)) we expect the star to evolve as if semiconvection was absent, where the edge of the convection zone is this time determined by the Ledoux criterion.

When semiconvection is enabled in the model, material can be exchanged between the convective core and surrounding regions. This results in a competition between nuclear burning, which maintains the composition gradient, and semiconvective mixing, which tries to remove the gradient. We can therefore estimate  $H_{L,\text{crit}}$  by comparing the mixing timescale of the semiconvective region to the compositional evolution timescale in the convective core. The semiconvective mixing timescale is given by

$$t_{\text{semi}} = \frac{l_{\text{semi}}^2}{\langle D_{\text{semi}} \rangle}, \quad (29)$$

where  $l_{\text{semi}}$  is the radial extent of the entire semiconvective region and  $\langle D_{\text{semi}} \rangle$  is the mass-averaged diffusion coefficient in the semiconvective region. Similarly, we can compute the compositional change timescale as

$$t_{\mu,\text{center}} = \left| \frac{\mu_{\text{center}}}{\dot{\mu}_{\text{center}}} \right|, \quad (30)$$

where  $\mu_{\text{center}}$  is the mean molecular weight of the material at the center of the star. This is the same as the  $\mu$ -evolution timescale for the entire convective core since it is fully mixed. Changing  $H_L$  affects the value of  $t_{\text{semi}}$ , but not  $t_{\mu,\text{center}}$ . The critical layer height is the value of  $H_L$  for which these two timescales are equal. Writing the diffusion coefficient (see Equation (27)) as

$$D_{\text{semi}} = D_{\text{semi},0} \left( \frac{H_L}{H_P} \right)^{1.48} \approx D_{\text{semi},0} \left( \frac{H_L}{H_P} \right)^{3/2}, \quad (31)$$

to factor out the dependence on  $H_L$ , we can then estimate  $H_{L,\text{crit}}$  by equating  $t_{\text{semi}}$  and  $t_{\mu,\text{center}}$ ,

$$H_{L,\text{crit}} \approx H_P \left( \frac{l_{\text{semi}}^2}{D_{\text{semi},0} t_{\mu,\text{center}}} \right)^{2/3}. \quad (32)$$

In order to estimate  $l_{\text{semi}}$ , we run a model under the Ledoux criterion and calculate where the boundary of the convective core would be were we to use the Schwarzschild criterion instead;  $l_{\text{semi}}$  is the distance between the actual Ledoux and hypothetical Schwarzschild convective boundaries.<sup>5</sup> Figure 5 shows the resulting time-averaged  $H_{L,\text{crit}}$  values over the main sequence evolution of stars in the mass range of  $1.2\text{--}3.0 M_\odot$ . Given that  $H_P \approx 10^{10}$  cm near the cores of such stars, we find

<sup>5</sup> This is the same as the size of semiconvective regions in models where chemical transport is turned off (e.g., by setting  $D_{\text{semi}} = 0$ ) or the layer heights used are small enough where mixing is inconsequential.



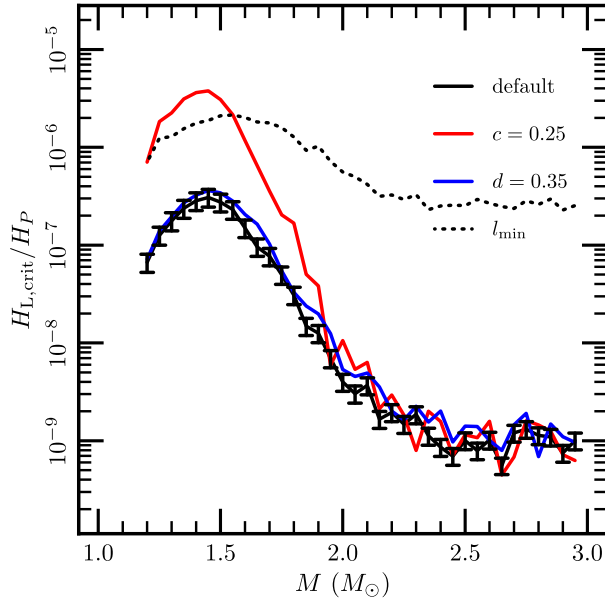


**Figure 5.** Estimates of the time-averaged critical layer height,  $H_{L,crit}$ , during main sequence evolution as a fraction of pressure scale height as a function of stellar mass. The black line represents critical layer height estimates using the fiducial fitting formula in Equation (18),  $\text{Nu}_\mu - 1 \propto \text{Ra}^c \text{Pr}^d$ , with  $c = 0.37$  and  $d = 0.25$ . Error bars correspond to the uncertainties in the fit,  $\Delta c = 0.04$  and  $\Delta d = 0.01$ . The red line corresponds to changing the fit so that  $\text{Nu}_\mu - 1$  scales as  $\text{Ra}^{0.25}$ , and the blue line corresponds to changing the fit so that  $\text{Nu}_\mu - 1$  scales as  $\text{Pr}^{0.35}$ . Semiconvective layer heights larger than  $H_{L,crit}$  will rapidly mix the semiconvective regions before the star evolves off the main sequence, destroying the chemical gradient that supports them and turning the region convective. Smaller layer heights will allow layered semiconvective regions to maintain their composition gradient and survive through the main sequence. For all masses considered here, the critical layer height is much smaller than the expected minimum layer height (shown in the dotted black line), which suggests that layered semiconvection cannot persist in main sequence stars and convective core evolution is therefore well approximated with that obtained under the Schwarzschild criterion.

that  $H_{L,crit}$  ranges from  $\approx 10^2$ – $10^3$  cm for stars in the mass range of greatest potential semiconvective impact, 1.2–1.7  $M_\odot$ .

While  $H_{L,crit}$  was determined from basic timescale arguments, we can easily compare it to the actual layer heights realized in numerical simulations.<sup>6</sup> Wood et al. (2013) found that the smallest layer heights are always observed just after the spontaneous onset of layer formation. In most of their simulations ran in boxes that are  $100d$  tall, the initial number of layers was 2 or 3, which implies an initial layer height between  $30d$  and  $50d$ —see their Table 1. We therefore have

$$l_{\min} \approx 30d = 30 \left( \frac{\kappa_{T\nu}}{g\delta \left| \frac{d \ln T}{dr} - \frac{d \ln T^{\text{ad}}}{dr} \right|} \right)^{1/4} \\ = 30 \left( \frac{P\kappa_{T\nu}}{\rho g^2 \delta |\nabla - \nabla_{\text{ad}}|} \right)^{1/4} \approx 10^4 \text{ cm}. \quad (33)$$

<sup>6</sup> We note that an estimate of the minimum layer height in layered semiconvection was attempted in Zaussinger & Spruit (2013), but they used the underlying instability length scale as a lower bound on the layer height (which it certainly is).

This implies that the minimum layer height is much larger than  $H_{L,crit}$  (see Figure 5). This has a fundamental consequence: layered semiconvection is so efficient in main sequence stars that it is accurately approximated by evolution under the Schwarzschild criterion, ignoring semiconvection altogether!

As mentioned in Section 2, the numerical simulations of Wood et al. (2013) covered Prandtl numbers down to  $10^{-2}$ , while stellar values are closer to  $10^{-5}$ . Therefore, the Nusselt numbers we use in our formulae for compositional and thermal fluxes, Equations (17) and (18), must be extrapolated down to much lower Pr. This creates some degree of uncertainty in the inferred fluxes for stellar parameters. We briefly investigate how this impacts our estimates of the critical layer height,  $H_{L,crit}$ . Since we use values of  $l_{\text{semi}}$  and  $t_{\mu,\text{center}}$  from Ledoux models, the relevant uncertainties are those in the extrapolation of the compositional flux, Equation (18). Wood et al. (2013) determined the power-law scalings of this flux with  $\text{Ra}^c$  and  $\text{Pr}^d$ , where  $c = 0.37 \pm 0.01$  and  $d = 0.27 \pm 0.04$ . We quantify the robustness of our critical layer height calculations by showing how much it changes if these powers themselves are different for very low Pr. Figure 5 shows the resulting  $H_{L,crit}$  values obtained with different scaling laws. The power of Ra has a much larger impact on  $H_{L,crit}$  than the power of Pr. Decreasing the exponent on Ra gives a lower value for  $D_{\text{semi}}$  for a given layer height, and thus less efficient semiconvective mixing. Since the semiconvective mixing timescale is now longer, then the critical layer height that makes  $t_{\text{semi}} = t_{\mu,\text{center}}$  must be larger. Decreasing the power of Ra down to 0.25 (from the fiducial 0.37) increases our estimated  $H_{L,crit}$  values, but they remain smaller than the minimum layer heights observed in the simulations of Wood et al. (2013) for most stellar masses.

Figure 6 illustrates the behavior of stellar models with layered semiconvection using Kippenhahn diagrams of a 1.3  $M_\odot$  star evolved with various mixing prescriptions. Although unphysically small, we first investigate the effect of layered semiconvection using layer heights  $H_L \ll H_{L,crit}$ . As expected, we find that semiconvective regions are effectively radiative and the star evolves as if semiconvection was ignored altogether, with the edge of the convection zone given by the Ledoux criterion. For the more realistic case where  $H_L \gg H_{L,crit}$ , the evolution is nearly identical to the Schwarzschild case, as predicted above. Our results also highlight how sensitive core evolution is to the layer height. There are several orders of magnitude difference in  $H_L$  between models that are effectively the same as the Schwarzschild case and models that are effectively the same as the Ledoux case. Intermediate values of  $H_L$  initially have semiconvection zones extending out to where the Schwarzschild convective boundary would be, which eventually transition into convective zones (under the Ledoux criterion) before core hydrogen depletion.

Figure 7 summarizes the convective core evolution for several different mixing criteria, showing that it falls into three size groups. The smallest convective cores occur when smoothing is enabled, and semiconvective mixing is either turned off or is weak enough ( $H_L \ll H_{L,crit}$ ) that the evolution is effectively the same as a Ledoux model. Convective cores are larger for the same cases if smoothing is not used. Finally, the largest convective cores occur for efficient semiconvection (the only physically realizable outcome, where  $H_L \gg H_{L,crit}$ ) and is nearly identical to the Schwarzschild case. For these models, turning on smoothing does not have a noticeable effect due to the strong mixing outside the convective boundary.

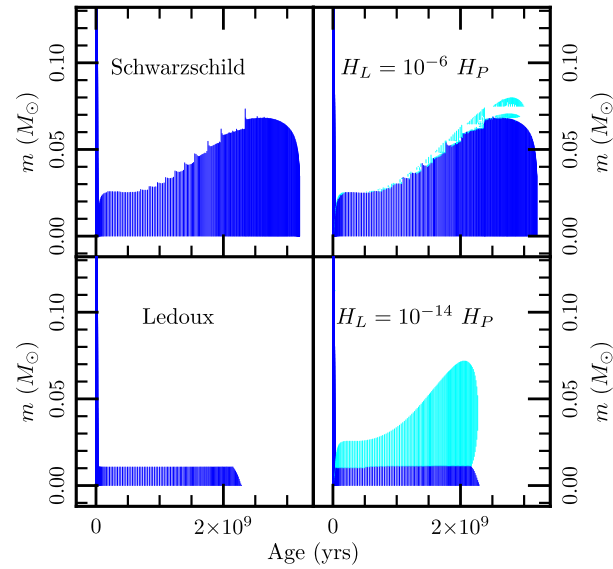


**Figure 6.** Kippenhahn diagrams for the main sequence evolution of a  $1.3 M_{\odot}$  star using different mixing criteria. The panels on the left show the evolution of the convective core (blue) under the Schwarzschild and Ledoux criteria. The convective core is much smaller in the Ledoux case because there is a significant stabilizing composition gradient outside the core due to pp-chain burning. The main-sequence lifetime of this case is therefore significantly shorter. The panels on the right show the corresponding evolution with layered semiconvection using layer heights many orders of magnitude larger and smaller than the critical layer height,  $H_{L,crit} \approx 10^{-8} H_P$ . The core evolution of the larger  $H_L$  case is virtually the same as one obtained with a model using the Schwarzschild criterion, while the evolution under the smaller  $H_L$  case is virtually the same as the Ledoux case. Only the  $H_L \ll H_{L,crit}$  model shows large semiconvective zones (light blue) over the entirety of the main sequence, because the mixing is too slow to remove the composition gradient.

Finally, we show that the same results hold in models with convective overshoot. We are not addressing the question of whether standard overshooting prescriptions should be used with semiconvection. Indeed, there are likely modifications to overshooting prescriptions in the presence of chemical gradients (see e.g., Canuto 1998). Instead, we show that our scheme for layered semiconvection can be combined with overshooting without causing numerical problems as a check that the overall behavior is not unduly sensitive to the presence of other types of mixing beyond the convective region. Figure 8 shows the evolution of a pure Schwarzschild model, a Schwarzschild model with overshoot, and a semiconvective model with  $H_L \gg H_{L,crit}$  (thus effectively as if it were run with the Schwarzschild criterion). We see that the semiconvective models that are effectively Schwarzschild models remain so with convective overshoot, so the respective prescriptions combine without issue. We also note that, as expected, the spikiness of the convective core mass under Schwarzschild evolution can be removed with a small amount of convective overshoot.

## 5. CONCLUSION

Convective core evolution of main sequence stars in the mass range  $1.2\text{--}1.7 M_{\odot}$  can be dramatically impacted by semiconvective mixing due to the extended composition gradient outside the convective boundary coming from nuclear burning. We investigated the effects of the layered

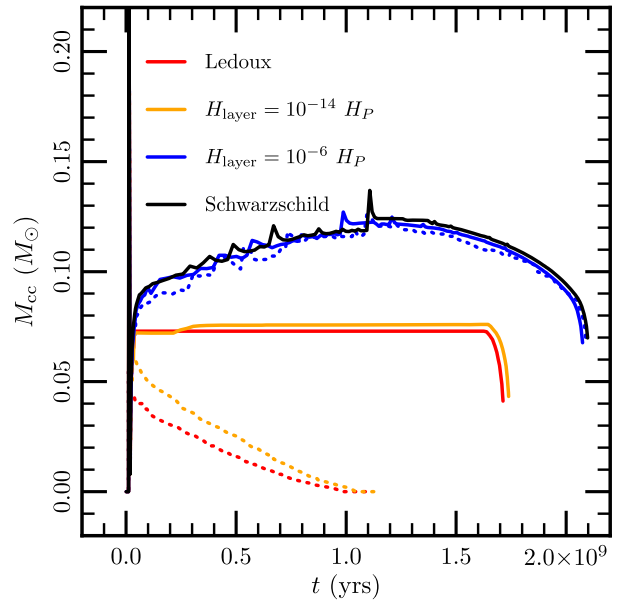


**Figure 7.** Main sequence evolution of the convective core mass,  $M_{cc}$ , for  $1.5 M_{\odot}$  stars under various mixing schemes. Dashed lines indicate the same mixing parameters as solid lines, but with the default 7-point Gaussian  $\nabla_{\mu}$ -smoothing enabled. By adjusting the convection criterion, smoothing, and strength of layered semiconvection, the convective core evolution falls into roughly three cases. The smallest convective cores occur when the Ledoux criterion (or layered semiconvection with  $H_L \ll H_{L,crit}$ ) is used in conjunction with  $\nabla_{\mu}$ -smoothing. Mid-size convective cores occur for the same cases but without  $\nabla_{\mu}$ -smoothing enabled. The largest convective cores occur with either the Schwarzschild criterion or with layered semiconvection where  $H_L \gg H_{L,crit}$ . For those cases, it does not matter whether or not  $\nabla_{\mu}$ -smoothing is enabled, since the mixing is strong enough to destroy composition gradients.

semiconvection prescription given in Wood et al. (2013) on the evolution of such stars. We found that there is a critical layer height,  $H_{L,crit}$ , above which the core evolution is nearly the same as in models which ignore composition gradients altogether, evolving the star using the Schwarzschild criterion. For layer heights smaller than  $H_{L,crit}$ , the semiconvective mixing beyond the convective core is effectively irrelevant and the star evolves as if the Ledoux criterion was used. This critical layer height is orders of magnitude smaller than the minimum layer height predicted from the underlying instability, so if layered semiconvection occurs within stars, we expect it to be very effective at mixing composition and quickly erasing the composition gradient that allows it to exist. We therefore conclude that the effect of semiconvection on convective core evolution is reasonably well captured by simple models that use the Schwarzschild criterion to locate the edge of convective regions.

We also found that numerically smoothing the composition gradient term can significantly change the sizes of convective cores. When using the Ledoux criterion, this  $\nabla_{\mu}$ -smoothing will artificially push the convective core boundary inward, shrinking the convective core. This effect can be dramatic if no additional mixing is included beyond the convection zone, and can artificially reduce the lifetimes of evolutionary phases with convective cores by up to 50%.

Our results on the convective core evolution of main sequence stars with layered semiconvection suggest that the minimum convective core size can be estimated by using the

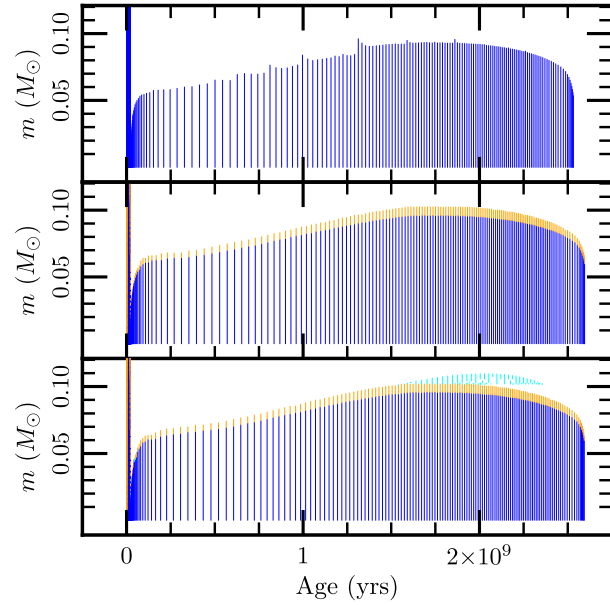


**Figure 8.** Kippenhahn diagrams for the main sequence evolution of a  $1.4 M_{\odot}$  star showing the effects of overshoot on smoothing out the temporal evolution of the convective core. Dark blue regions are convective, light blue regions are semiconvective, and orange regions correspond to overshooting. The top panel shows the evolution under the Schwarzschild criterion. The middle panel shows the same evolution but also with overshoot turned on (using  $f = f_0 = 10^{-4}$ ). The bottom panel shows evolution with layered semiconvection at a value of  $H_l = 10^{-6} H_p$  and the same overshooting parameters.

Schwarzschild criterion, ignoring semiconvection altogether. This conclusion is similar to one of the conclusions of Gabriel et al. (2014), although arrived at for different reasons.

Thanks to the excellent data sets provided by missions such as *KEPLER* and *CoRoT*, it is now possible to infer the sizes of convective cores in main sequence stars from observations of pulsation modes (Mazumdar et al. 2006; Cunha & Metcalfe 2007; Silva Aguirre et al. 2010a; Brandão et al. 2014). It may even be possible in the future to detect layered convection directly (Belyaev et al. 2015). Sample sizes of solar-like oscillators (both main sequence stars and sub giants) are currently only in the dozens (Appourchaux et al. 2012; Metcalfe et al. 2014). Furthermore, inferences of the convective core size have been performed on only a handful of these stars (Silva Aguirre et al. 2013; Liu et al. 2014; Deheuvels 2015). This limited sample shows evidence of mixing beyond the Schwarzschild convection boundary, typically interpreted as a constraint on the amount of overshooting. As discussed above, this is consistent with our predictions on convective core sizes. It also suggests that it may not be possible to place constraints on the strength of layered semiconvection in main sequence stars from measurements of the core size alone. A more fruitful approach may either be to focus on stars that have faster evolutionary timescales, or that contain large semiconvective zones that are detached from the convective core (e.g., higher mass and/or more evolved stars). We are planning a future paper to examine this prospect.

We thank Justin Brown, Jonathan Fortney, Chris Mankovich, Nadine Nettelmann, and Bill Paxton for useful

discussions. Code and inlists necessary to reproduce our models are hosted on mesastar.org. This work was supported under grants NSF AST 0847477 and NSF AST 1211394.

## REFERENCES

- Appourchaux, T., Chaplin, W. J., García, R. A., et al. 2012, *A&A*, **543**, A54
- Baines, P. G., & Gill, A. E. 1969, *JFM*, **37**, 289
- Belyaev, M. A., Quataert, E., & Fuller, J. 2015, *MNRAS*, **452**, 2700
- Böhm-Vitense, E. 1958, *ZAp*, **46**, 108
- Brandão, I. M., Cunha, M. S., & Christensen-Dalsgaard, J. 2014, *MNRAS*, **438**, 1751
- Canuto, V. M. 1998, *ApJL*, **508**, L103
- Canuto, V. M. 1999, *ApJ*, **524**, 311
- Crowe, R. A., & Mitalas, R. 1982, *A&A*, **108**, 55
- Cunha, M. S., & Metcalfe, T. S. 2007, *ApJ*, **666**, 413
- Deheuvels, S. 2015, Cambridge Workshop on Cool Stars, Stellar Systems, and the Sun, Vol. 18, ed. G. T. van Belle & H. C. Harris, **489**
- Ding, C. Y., & Li, Y. 2014, *MNRAS*, **438**, 1137
- Faulkner, D. J., & Cannon, R. D. 1973, *ApJ*, **180**, 435
- Gabriel, M., & Noels, A. 1977, *A&A*, **54**, 631
- Gabriel, M., Noels, A., Montalbán, J., & Miglio, A. 2014, *A&A*, **569**, A63
- Garaud, P. 2013, in *New Advances in Solar Physics: From Microscopic to Macroscopic Processes*, Vol. 63, ed. G. Alecian et al. (Les Ulis: EDP Sciences), 285
- Garaud, P., Medrano, M., Brown, J. M., Mankovich, C., & Moore, K. 2015, *ApJ*, **808**, 89
- Georgy, C., Saio, H., & Meynet, G. 2015, in *IAU Symp., Vol. 307, New Windows on Massive Stars: Astro-seismology, Interferometry, and Spectro Polarimetry* (Cambridge: Cambridge Univ. Press), 47
- Grossman, S. A., & Taam, R. E. 1996, *MNRAS*, **283**, 1165
- Joseph, D. D. 1966, *ArRMA*, **22**, 163
- Kato, S. 1966, *PASJ*, **18**, 201
- Kippenhahn, R., Weigert, A., & Weiss, A. 2012, *Stellar Structure and Evolution* (Berlin: Springer)
- Langer, N. 1991, *A&A*, **252**, 669
- Langer, N., El Eid, M. F., & Fricke, K. J. 1985, *A&A*, **145**, 179
- Langer, N., Fricke, K. J., & Sugimoto, D. 1983, *A&A*, **126**, 207
- Langer, N., & Maeder, A. 1995, *A&A*, **295**, 685
- Ledoux, P. 1947, *ApJ*, **105**, 305
- Liu, Z., Yang, W., Bi, S., et al. 2014, *ApJ*, **780**, 152
- Mazumdar, A., Basu, S., Collier, B. L., & Demarque, P. 2006, *MNRAS*, **372**, 949
- Merryfield, W. J. 1995, *ApJ*, **444**, 318
- Metcalfe, T. S., Creevey, O. L., Doğan, G., et al. 2014, *ApJS*, **214**, 27
- Mirouh, G. M., Garaud, P., Stellmach, S., Traxler, A. L., & Wood, T. S. 2012, *ApJ*, **750**, 61
- Moll, R., Garaud, P., & Stellmach, S. 2015, arXiv:1506.07900
- Paxton, B., Bildsten, L., Dotter, A., et al. 2011, *ApJS*, **192**, 3
- Paxton, B., Cantiello, M., Arras, P., et al. 2013, *ApJS*, **208**, 4
- Paxton, B., Marchant, P., Schwab, J., et al. 2015, *ApJS*, **220**, 15
- Proctor, M. R. E. 1981, *JFM*, **105**, 507
- Radko, T. 2003, *JFM*, **497**, 365
- Radko, T. 2013, *Double-diffusive Convection* (Cambridge: Cambridge Univ. Press)
- Robertson, J. W., & Faulkner, D. J. 1972, *ApJ*, **171**, 309
- Rosenblum, E., Garaud, P., Traxler, A., & Stellmach, S. 2011, *ApJ*, **731**, 66
- Sakashita, S., & Hayashi, C. 1961, *PThPh*, **26**, 942
- Schwarzschild, M., & Härm, R. 1958, *ApJ*, **128**, 348
- Silva Aguirre, V., Ballot, J., Serenelli, A., & Weiss, A. 2010a, arXiv:1004.2928
- Silva Aguirre, V., Ballot, J., Serenelli, A., & Weiss, A. 2010b, *Ap&SS*, **328**, 129
- Silva Aguirre, V., Ballot, J., Serenelli, A. M., & Weiss, A. 2011, *A&A*, **529**, A63
- Silva Aguirre, V., Basu, S., Brandão, I. M., et al. 2013, *ApJ*, **769**, 141
- Soderlund, K. M., Heimpel, M. H., King, E. M., & Aurnou, J. M. 2013, *Icar*, **224**, 97
- Spruit, H. C. 1992, *A&A*, **253**, 131
- Spruit, H. C. 2013, *A&A*, **552**, A76
- Stevenson, D. J. 1979, *MNRAS*, **187**, 129
- Stothers, R. 1970, *MNRAS*, **151**, 65

Stothers, R., & Chin, C.-W. 1975, [ApJ](#), 198, 407  
Sukhbold, T., & Woosley, S. E. 2014, [ApJ](#), 783, 10  
Turner, J. S. 1973, *Buoyancy Effects in Fluids* (Cambridge: Cambridge Univ. Press)

Weiss, A., Hillebrandt, W., Thomas, H.-C., & Ritter, H. 2004, *Cox and Giuli's Principles of Stellar Structure* (Cambridge: Princeton Publishing Associates)  
Wood, T. S., Garaud, P., & Stellmach, S. 2013, [ApJ](#), 768, 157  
Zaussinger, F., & Spruit, H. C. 2013, [A&A](#), 554, A119